

1                   *Supplement of* “**Hot spots, hot moments, and**  
2                   **spatiotemporal drivers of soil CO<sub>2</sub> flux in temperate**  
3                   **peatlands using UAV remote sensing**”

4                   **Yanfei Li<sup>1,\*</sup>, Maud Henrion<sup>1</sup>, Angus Moore<sup>1</sup>, Sébastien Lambot<sup>1</sup>, Sophie**  
5                   **Opfergelt<sup>1</sup>, Veerle Vanacker<sup>1</sup>, François Jonard<sup>2,†</sup>, Kristof Van Oost<sup>1,†</sup>**

6                   <sup>1</sup> Earth and Life Institute, Université catholique de Louvain, 1348 Louvain-la-Neuve, Belgium

7                   <sup>2</sup> Earth Observation and Ecosystem Modelling Laboratory, Université de Liège, 4000 Liège, Belgium

8                   <sup>†</sup> These authors are co-last authors

9                   \*Corresponding author. E-mail: yanfei.li@uclouvain.be (Yanfei Li). Present address: Place Louis Pasteur  
10                  3, 1348 Louvain-la-Neuve, Belgium.

### Text S1: Daily soil temperature mapping

The linear mixed-effects model was utilized to predict the spatial distribution of daily mean soil temperature (10 cm depth) across the landscape from 1 May 2023 to 30 April 2024. Daily mean air temperature, Normalized Difference Vegetation Index (NDVI) and Land Surface Temperature (LST) were considered as fixed-effect predictors and monitoring sites were included as random effects. The model was performed using the *lmer function* of the *lme4 package* and was defined as:

$$y_{ij} = \beta_0 + \beta_1 x_{ij} + \dots + \beta_p x_{ij} + b_{0j} + b_{1j} z_{ij} + \dots + \epsilon_{ij} \quad (5)$$

Where:

- $y_{ij}$  is the dependent variable (i.e., soil temperature at 10 cm, unit: °C) for observations  $i$  in group  $j$ .
- $\beta_0, \beta_1, \dots, \beta_p$  are fixed-effect coefficients.
- $x_{ij}$  indicates fixed-effect predictors (independent variables).
- $b_{0j}, b_{1j}, \dots$  are random-effect coefficients associated with group  $j$ , which account for variability across groups.
- $z_{ij}$  indicates predictors associated with random effects.
- $\epsilon_{ij}$  is the residual error term.

Soil temperature data were collected from both Teros 12 sensors and data loggers, as described in Section 2.3. Air temperature measurements were obtained from five stations positioned at different slope locations. The NDVI and LST estimates were extracted from maps by retrieving values at the 20 soil temperature sensor sites. These sites were included as random effects in the model to account for repeated measurements at the same locations throughout the monitoring period.

For mapping purposes, daily air temperature was upscaled by incorporating the relationship between air temperature and elevation, followed by upscaling using a Digital Terrain Model (DTM) derived from LiDAR data. The daily NDVI and LST maps were generated by linearly interpolating the monthly/biweekly maps derived from UAVs. The model training, testing, and evaluation procedures followed the methodology outlined in Section 2.6.2. Model coefficients and performance on the training dataset is summarized in Table S2, while Figure S2 illustrates the modelled versus observed soil temperatures.

## Text S2: Generation of corrected daily TWI

We generated corrected daily TWI maps to approximate the spatial distribution of soil volumetric water content (VWC) by incorporating both long-term site characteristics and daily precipitation effects. First, we calculated the mean VWC for each site over the period from 1 May 2023 to 30 April 2024. Then, we extracted each site's TWI values from a TWI map generated using the formula in Table S1. Next, we performed a linear regression with mean VWC as the response and TWI as the predictor:

$$Baseline = Mean\ VWC = b + a * TWI \quad (1)$$

The *Baseline* represents the soil moisture level at long-term. A baseline map was then created using this regression model. Daily deviations (anomalies) from the baseline were defined as:

$$Anomaly_t = VWC_t - Baseline \quad (2)$$

Considering the memory and lag effects in soil moisture dynamics, we assumed that the anomaly on any day is influenced by the previous day's anomaly and rainfall:

$$Anomaly_t = c * Anomaly_{t-1} - d * Rainfall_{t-1} \quad (3)$$

Finally, we generated a “corrected TWT” map for each day by adding the dynamically updated anomaly to the baseline map:

$$Corrected\ TWI_t\ map = Baseline\ map + Anomaly_t \quad (4)$$

This approach allows the daily corrected TWI maps to capture both the inherent spatial variability (as determined by TWI) and the dynamic influence of rainfall, thereby serving as a proxy for the spatial distribution of soil moisture.

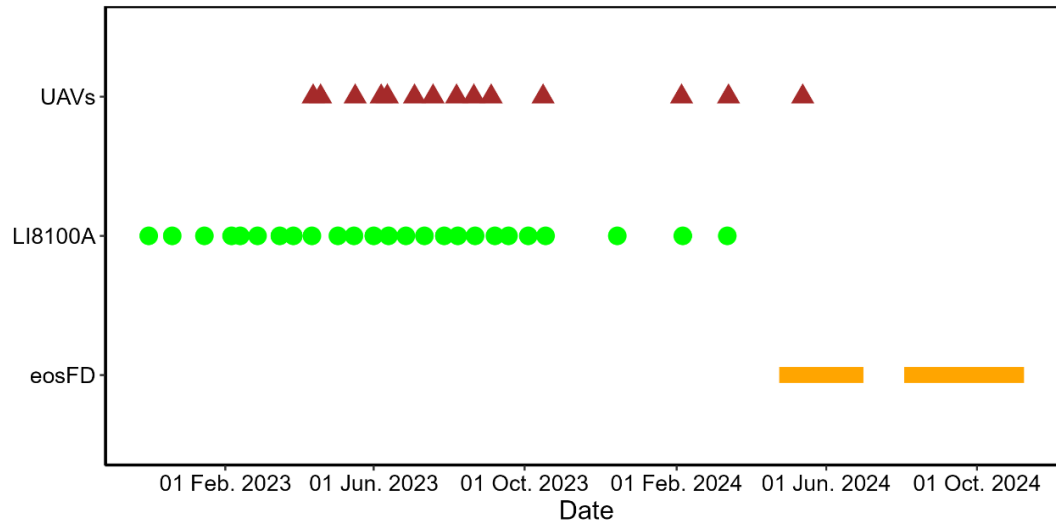


**Figure S1.** Dates of UAV flight missions, CO<sub>2</sub> flux measurements using the LI8100A system, and CO<sub>2</sub> flux measurements using the eosFD probes.

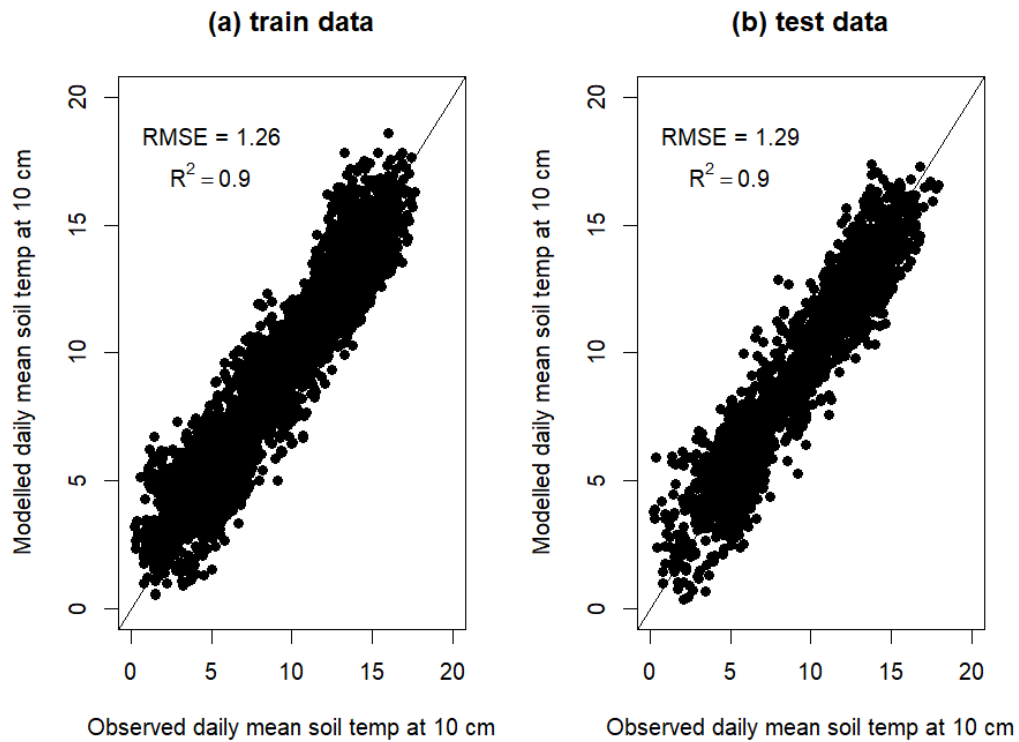
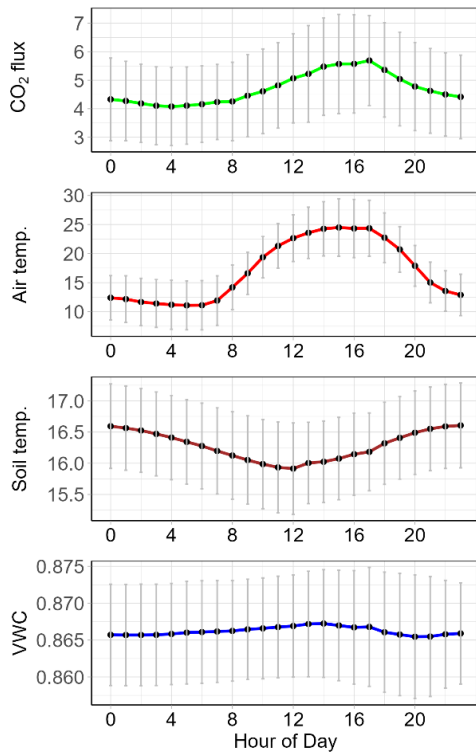
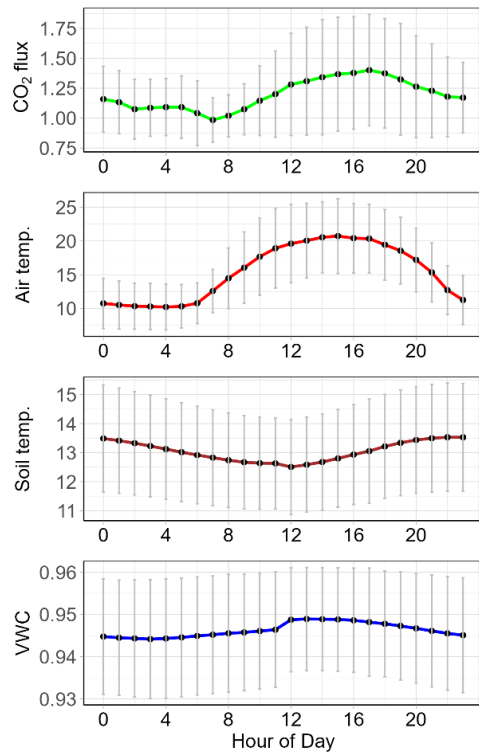


**Figure S2.** Estimated daily mean soil temperature (at 10 cm depth) against observations using linear mixed-effects model. The corresponding *RMSE* and *R*<sup>2</sup> values for the train and test datasets are annotated on the plot.

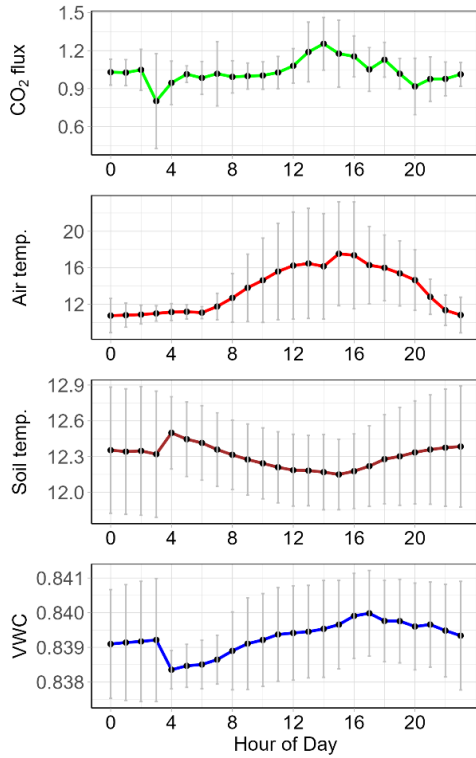
(a) Foothslope (03 Aug. - 27 Aug.)



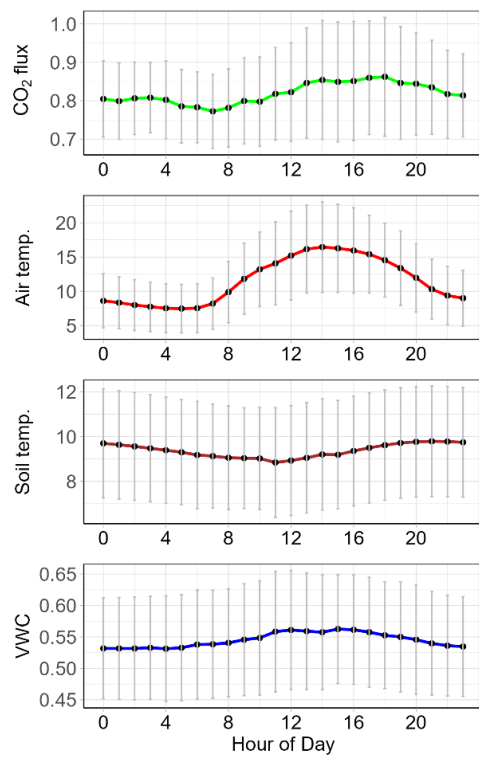
(b) Backslope (11 Jun. - 01 Jul.)



(c) Shoulder\_wet (13 May - 18 May)



(d) Shoulder\_dry (24 Apr. - 13 May)



70

71

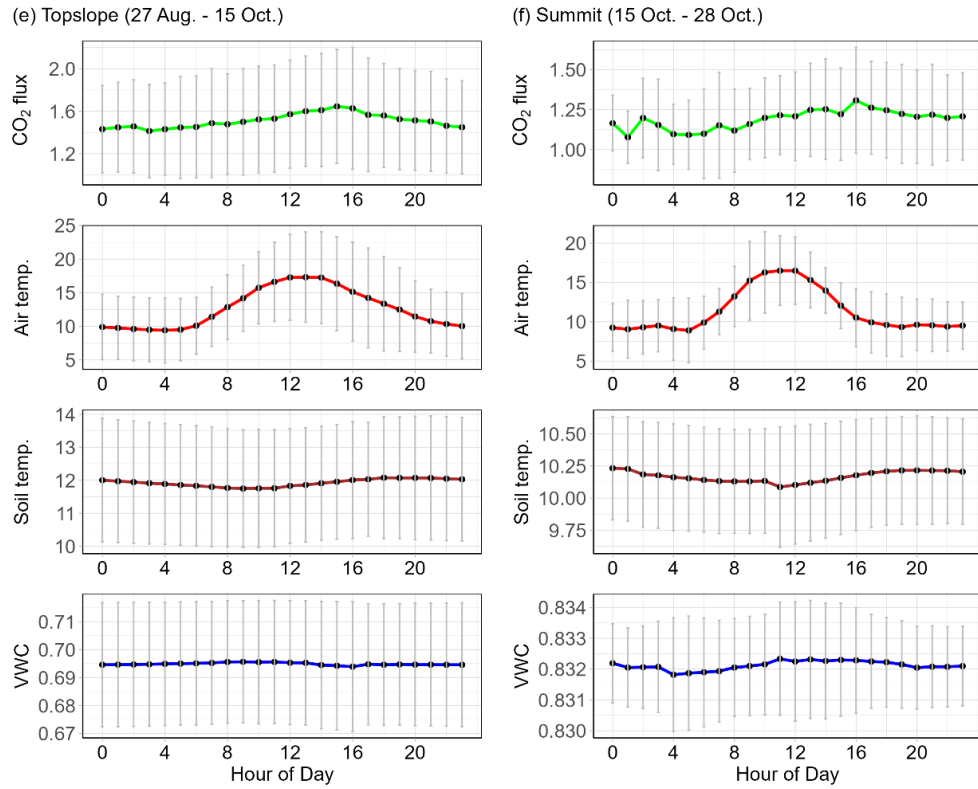


**Figure S3.** Mean hourly CO<sub>2</sub> flux, air temperature (Air temp.), soil temperature (Soil temp.), and VWC across different slope positions. The CO<sub>2</sub> data (unit:  $\mu\text{mol m}^{-2} \text{s}^{-1}$ ) based on measurements from the eosFD probes. Soil temperature (unit:  $^{\circ}\text{C}$ ) and VWC ( $\text{cm}^3 \text{cm}^{-3}$ ) were monitored at a depth of 10 cm using the Teros12 sensors. The air temperature (unit:  $^{\circ}\text{C}$ ) was monitored at  $\sim 1.4$  m above ground. The dot indicates the mean value, and the grey line (error bar) indicates the sd of each hour. The numbers of each subplot title indicate the monitoring period (Month/day).

**Table S1.** Orthorectified image, topographical, vegetation index, and land surface temperature maps derived from RGB, LiDAR, multispectral and thermal images.

Index	Definition	Unit	Data source
RGB orthomosaic	Orthorectified image mosaicked from RGB image collection	/	RGB
DTM	Digital Terrain Model	m	LiDAR
TWI	Terrain wetness index: $\ln (As/\tan(b))$ , where $As$ is the specific contributing area and $b$ is the slope angle in radians.	/	LiDAR
NDVI	Normalized Difference Vegetation Index: $(near\ infrared - red) / (near\ infrared + red)$	/	Multispectral
LST	Land Surface Temperature	°C	Thermal

**Table S2.** Coefficients and relative contributions of three input variables of linear mixed-effects regression models for modelling soil temperature. Random effects were evaluated by *ICC* and model performance was evaluated by *Marginal R<sup>2</sup>* and *Conditional R<sup>2</sup>*.

Fixed effects: Coefficients (contributions)	Air temperature	0.32*** (38.87 %)
	NDVI	5.58*** (27.84 %)
	LST	0.22*** (21.72 %)
Random effects	<i>ICC</i> (contributions)	0.19 (3.00 %)
Model performance	<i>Marginal R<sup>2</sup></i>	0.88
	<i>Conditional R<sup>2</sup></i>	0.91

Note. Significance level: \*\*\*  $p < 0.001$ , \*\*  $p < 0.01$ , \*  $p < 0.05$ .

**Table S3.** Summary of mean daily air temperature (Air temp.), soil temperature (Soil temp.), soil volumetric water content (VWC), soil subsurface properties at 10 cm depth, i.e, dry root biomass, soil organic carbon (SOC) content, total nitrogen (TN) content, and C/N ratio, under different slope positions.

Slope positions	Footslope	Backslope	Shoulder wet	Shoulder dry	Topslope	Summit
Vegetation	<i>Molinia caerulea</i>	<i>Vaccinium myrtillus</i>	<i>Juncus acutus</i>	<i>Molinia caerulea</i>	<i>Vaccinium myrtillus</i>	<i>Molinia caerulea</i>
Air temp. (°C)	8.89 ± 6.77 <sup>a</sup> (-8.76, 23.75)	9.56 ± 6.74 <sup>a</sup> (-7.68, 24.79)	9.61 ± 6.70 <sup>a</sup> (-7.77, 24.60)	N.A.	9.54 ± 6.76 <sup>a</sup> (-7.83, 24.66)	9.13 ± 6.86 <sup>a</sup> (-8.44, 24.52)
Soil temp. (°C)	9.56 ± 4.66 <sup>a</sup> (1.29, 17.48)	9.43 ± 4.32 <sup>a</sup> (1.40, 16.98)	9.55 ± 4.30 <sup>a</sup> (1.62, 16.74)	8.78 ± 4.17 <sup>a</sup> (0.75, 15.52)	8.73 ± 3.75 <sup>a</sup> (1.55, 15.18)	9.07 ± 4.12 <sup>a</sup> (1.82, 16.00)
VWC (cm <sup>3</sup> cm <sup>-3</sup> )	0.86 ± 0.06 <sup>b</sup> (0.68, 0.91)	0.94 ± 0.04 <sup>a</sup> (0.81, 0.98)	0.85 ± 0.01 <sup>c</sup> (0.83, 0.87)	N.A.	0.68 ± 0.08 <sup>c</sup> (0.44, 0.73)	0.82 ± 0.04 <sup>d</sup> (0.70, 0.85)
root biomass (g 100g <sup>-1</sup> )	1.43 ± 1.11 <sup>a</sup> (0.20, 3.37)	0.97 ± 0.87 <sup>a</sup> (0.27, 2.65)	4.02 ± 2.10 <sup>a</sup> (1.98, 6.17)	2.97 ± 3.00 <sup>a</sup> (0.70, 8.46)	0.98 ± 0.99 <sup>a</sup> (0.18, 2.84)	0.69 ± 0.27 <sup>a</sup> (0.31, 0.96)
SOC content (g 100g <sup>-1</sup> )	38.48 ± 1.71 <sup>ab</sup> (36.55, 40.8)	42.36 ± 2.46 <sup>a</sup> (37.6, 44.3)	47 ± 1.41 <sup>a</sup> (45.95, 48.6)	42.53 ± 2.51 <sup>a</sup> (39.75, 45.95)	32.26 ± 10.81 <sup>b</sup> (13.5, 42.1)	47.38 ± 2.06 <sup>a</sup> (43.95, 49.15)
TN content (g 100g <sup>-1</sup> )	2.22 ± 0.13 <sup>a</sup> (2.03, 2.37)	2.02 ± 0.11 <sup>ab</sup> (1.89, 2.16)	2.35 ± 0.17 <sup>a</sup> (2.16, 2.47)	2.04 ± 0.24 <sup>ab</sup> (1.71, 2.36)	1.61 ± 0.48 <sup>b</sup> (0.75, 2.19)	2.13 ± 0.14 <sup>a</sup> (1.99, 2.34)
C/N ratio	17.41 ± 1.57 <sup>b</sup> (15.59, 20.1)	20.98 ± 1.42 <sup>a</sup> (19.23, 22.70)	20.03 ± 1.26 <sup>ab</sup> (18.81, 21.32)	20.98 ± 1.95 <sup>a</sup> (18.6, 24.06)	19.76 ± 2.01 <sup>ab</sup> (18.08, 23.36)	22.32 ± 1.79 <sup>a</sup> (20.21, 24.51)

Note. The air temperature was monitored at a height of ~1.4 m above the ground. The soil temperature and VWC were monitored at a depth of 10 cm by Teros12 sensors. The results are presented as the mean ± sd and values in brackets indicate the minimum and maximum values. The *ANOVA* and *HSD* post-hoc tests were conducted within each class with the same superscript letters indicating no significant difference.